Integrated Modeling of NFIRAOS: Characterizing performance in the presence of vibration

Joeleff Fitzsimmons, David Andersen, Jenny Atwood,
Glen Herriot, Dan Kerley, Scott Roberts, Jean-Pierre Veran
National Research Council Canada – Herzberg Astronomy and Astrophysics
5071 West Saanich Road, Victoria, B.C. Canada, V9E 2E7

ABSTRACT

The Narrow Field InfraRed Adaptive Optics System (NFIRAOS) will be the first-light facility Multi-Conjugate Adaptive Optics (MCAO) system for the Thirty Meter Telescope (TMT). Historically, an important factor limiting the performance of an AO system has been the system vibrations and their impact on the delivered image quality. In order to leverage the extraordinary capabilities of the TMT, NFIRAOS must be capable of meeting the required optical performance and stability specifications while operating in the presence of the predicted vibration environments. Using the NRC-developed integrated modeling framework (NRCim), a detailed evaluation of the dynamic opto-mechanical performance of NFIRAOS was completed with several sources of structural disturbances (vibration from the telescope structure, from attached instruments, and internal to NFIRAOS). Multiple computational methodologies, including transient (time-series) and harmonic (transfer function) analyses combined with a Linear Optics Model (LOM), together with control system transfer functions for both common path and non-common-path disturbances were used to evaluate and compare the NFIRAOS delivered image quality. These procedures are described and the NFIRAOS performance in the presence of the various sources of vibration are reported. These sources include observatory vibration transmitted to NFIRAOS as well as internal sources such as the LGS WFS trombone, refrigeration, client instruments' rotator and cable wrap.

Keywords: Vibration, Integrated, modeling, NFIRAOS, TMT

1. INTRODUCTION

The Narrow Field InfraRed Adaptive Optics System (NFIRAOS) will be the first-light facility Multi-Conjugate Adaptive Optics (MCAO) system for the Thirty Meter Telescope (TMT). Historically, when measuring the success of an AO system, an important factor is the limitation of the AO system performance when subjected to real-world vibrations present in the observatory environment. There are many sources of vibration such as wind buffeting, telescope tracking jitter, cryogenic/coolant pumps and even mechanical components internal to a particular AO system. These, combined with other vibrations, lead to dynamic system instabilities that can result in a significant reduction in delivered image quality, sky coverage, optical throughput, angular resolution and astrometry.

The AO system sensitivity to vibration becomes increasingly important with larger telescopes since the diffraction limit of the telescope is inversely proportional to the telescope primary mirror diameter. Mounted on the TMT with a 30 meter diameter primary mirror, NFIRAOS will be required to deliver diffraction limited performance in J, H, and K bands in order to leverage the extraordinary capabilities of the TMT. Described in terms of allowable image degradation, NFIRAOS will deliver images with less than 187nm and 203nm RMS wave front error (WFE) when evaluated on axis and at 34 arcsec diameter, respectively.

Given these challenging performance requirements, the large physical size, and the significant cost for NFIRAOS, a comprehensive effort was launched to conduct detailed opto-mechanical analyses to minimize these risks. Building on the extensive development of the National Research Council Integrated Modeling (NRCim) toolset, the team at the Herzberg Astronomy and Astrophysics Research Centre (HAA) completed extensive analyses of the NFIRAOS instrument which are detailed in this report.

1.1 NRCim description

The NRCim framework is a highly configurable analysis toolset which can be applied to a wide variety of opto-mechanical system and is easily implemented using standard procedures and interfaces for configuring models. The block diagram shown in Figure 1 illustrates the interaction between the core NRCim code, implemented in MATLAB, and the structural and optical analysis software, ANSYS and ZEMAX, respectively. The NRCim framework includes a bidirectional interface to ZEMAX from MATLAB via Dynamic Data Exchange (DDE) and facilitates the manipulation of the optical prescription parameters including surface displacements, raytracing and other optical computations. A summary of the NRCim analysis process is as follows:

- A subset of nodes within the ANSYS FEM are defined with component names (a method within ANSYS used to identify a set of geometry) to represent the optical elements.
- Corresponding ZEMAX surfaces are identified with labels in the comment field which are stored, along with interface information and coordinate systems, in the MATLAB database.
- These associations are constructed once during the NRCim model initialization and stored in the database for future analysis runs. All coordinate systems can be independently defined since NRCim manages all the required transformations between analysis tools.
- A static disturbance (temperature, force, displacement, etc.) is defined in the ANSYS structural FEM and the structural displacements are transferred to ZEMAX for evaluation of the final image WFE.

The inner workings and initialization of the NRCim are detailed in Ref. [1].

The NRCim toolset has been applied to many problems already including the design optimization of the Canadian Very Large Optical Telescope (VLOT) [1] [2], the analysis of the TMT telescope structural model [3] [4], and the characterization of the Gemini Planet Imager (GPi) performance [5].

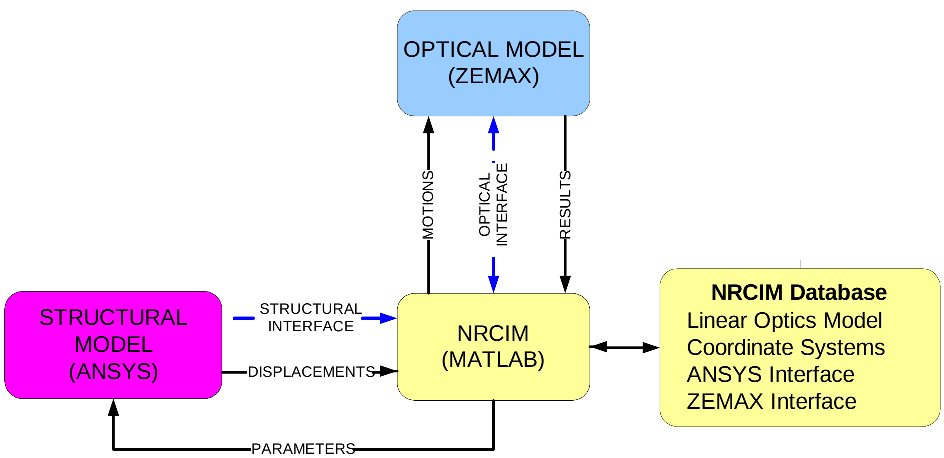

Figure 1. NRCim Framework Description

2. STATIC ANALYSES OF NFIRAOS USING NRCIM

2.1 NFIRAOS system overview

An isometric view of NFIRAOS is illustrated in Figure 2 showing NFIRAOS positioned on the TMT –X Nasmyth platform with the Infrared Imaging Spectrograph (IRIS) shown (in grey) suspended below. The NFIRAOS Instrument Support Tower (IST – the light blue structure) supports the NFIRAOS thermal enclosure (ENCL – shown in medium blue), the NFIRAOS optical table (TABL – not visible since it is inside the ENCL), up to three client instruments, and the NFIRAOS Science Calibration Unit (NSCU – not visible in this view). Shown in dark blue to the left of the Nasmyth platform is telescope elevation journal with the primary mirror located further to the left. The telescope structure (TEL.STR – shown in brown) is the structure that supports NFIRAOS above the Nasmyth platform. The “pitch & yaw” adjusters (shown in dark orange) are provided by the telescope structure and form the main mechanical interface between the TEL.STR and NFIRAOS.

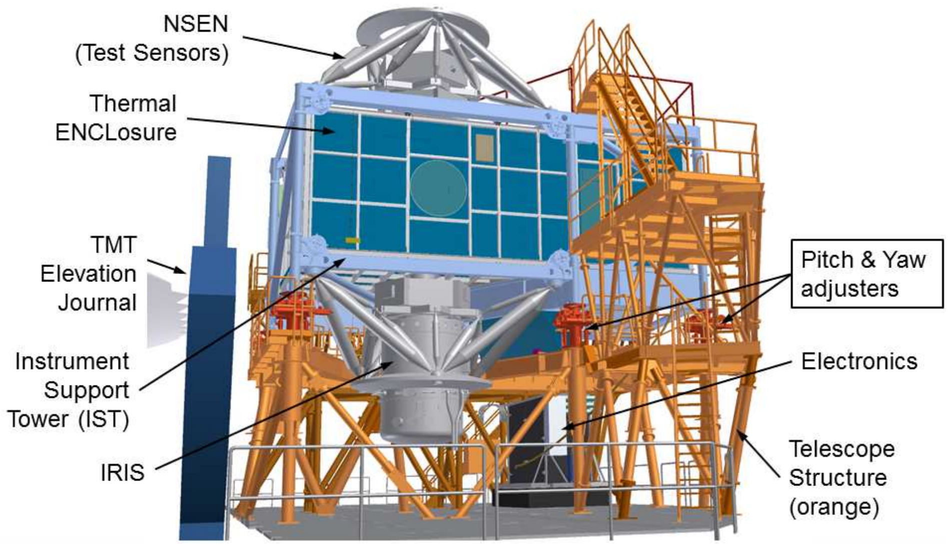

Figure 2. Assembly view of NFIRAOS with instruments, mounted on the TMT telescope structure.

The TABL is supported by the IST via three thermal isolation stubs that protrude through the ENCL floor. This allows the TABL and all the opto-mechanical components attached (see isometric view shown in Figure 3) to be maintained at -30±0.5˚C while structurally supported by the IST. Each of the opto-mechanical components are represented in the structural FEM and the optical prescription, shown in the top-right and bottom-right of Figure 3, respectively. For all static NRCim analyses, each subsystem was represented by a lumped mass located at the center of mass for each subsystem and connected to the TABL via rigid link elements to minimize any addition of local stiffness.

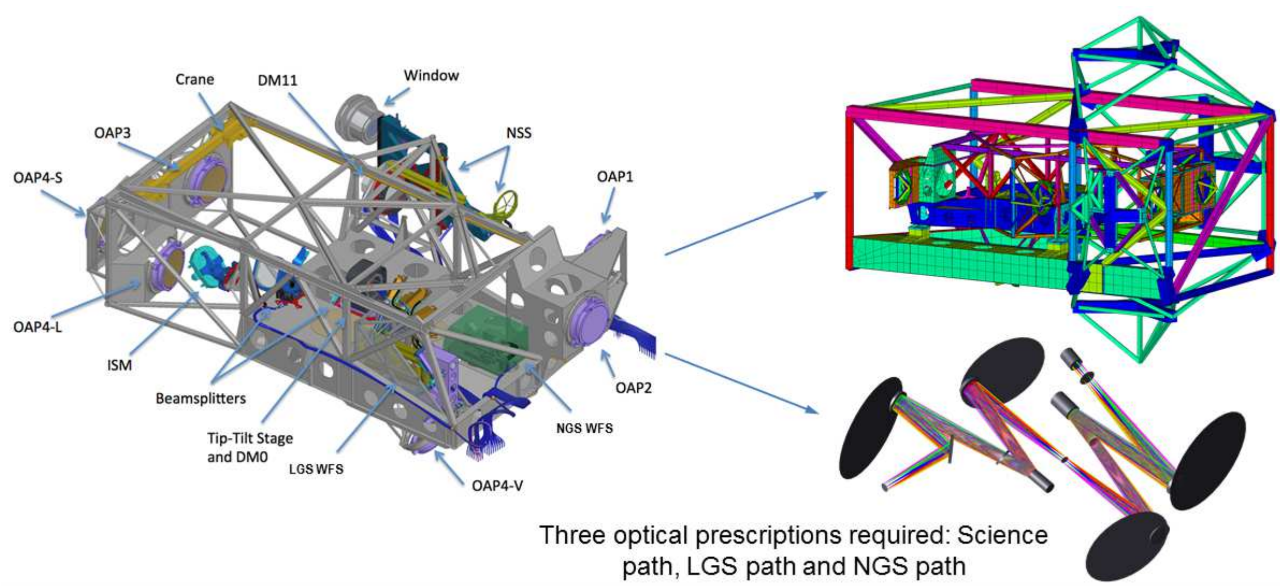

Figure 3. NFIRAOS TABL and sub-system decomposition to the FEM and ZEMAX representations

2.2 NFIRAOS NRCim – Interface Alignment Sensitivity Analyses

One of the first static NRCim analyses completed was to assess the TEL.STR-to-NFIRAOS interface alignment sensitivity. The integration and test plan developed for NFIRAOS involves the assembly, alignment and test of the entire system in Victoria, B.C., Canada before disassembly and shipment to the TMT site for assembly, integration and verification (AIV). The TEL.STR-to-NFIRAOS interface will be surveyed prior to assembly and alignment at both the I&T and site facilities. The final step in the AIV plan at the TMT site will be to adjust the "pitch & yaw" adjusters (shown in orange in Figure 2) to align the incoming beam with NFIRAOS. However, there will be some residual non-coplanarity of the six TEL.STR-to-NFIRAOS interface points with unknown impact to the overall performance of NFIRAOS.

NRCim was used to assess the sensitivity of the image quality and alignment to changes in the vertical position of each TEL.STR-to-NFIRAOS interface point. Incrementally, each of the six interface points (illustrated in Figure 4 below) were displaced vertically by 1 mm and the resulting FEM displacements were calculated (see Figure 5). Due to the close proximity of the TABL supports to the interface points 1, 4 and 5, perturbations of these three interface points resulted in significant TABL motion while the other three interface points had little impact. The displacements for all six cases were then processed through ZEMAX using NRCim to produce six perturbed prescriptions.

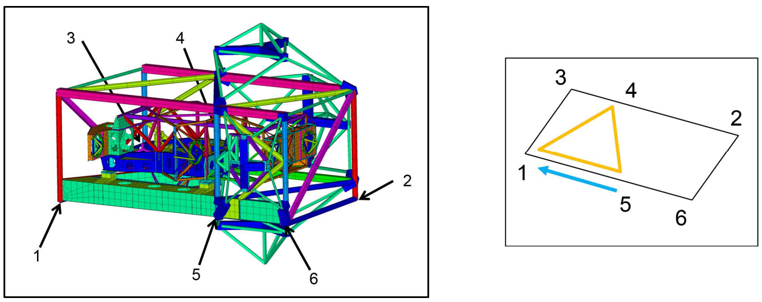

Figure 4. NF-STR interface layout and association with TABL support points (yellow triangle).

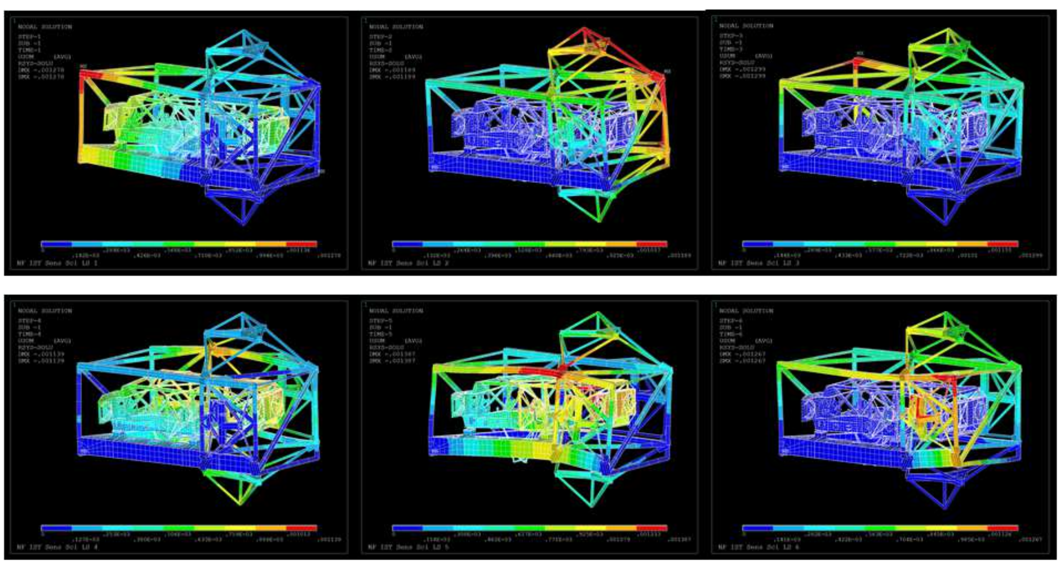

Figure 5. Six deformed FEM results for the NF-STR interface sensitivity analysis.

When assessing the impact of each of these perturbations, there were several compensators internal to NFIRAOS and in TMT that could be used to minimize various effects. Considering the possible compensators, the six prescriptions were optimized to minimize the interface alignment sensitivity. The optical performance parameters are tabulated in Table 1 showing that only cases 1 and 5 require the use of some DM stroke to correct for astigmatism. The results from these analyses were used to define the adjustment resolution requirements for the six adjustment actuators that will be used to control the 6-dof position of NFIRAOS.

Table 1. NRCim results for NF-STR IF sensitivity analysis.

Case #	IQ RMS Wavefront at 5 field points (nm RMS)					Focal Plane Mask Motion (mm)		Pupil Shift (mm/% of pupil)		Image Plane Motion (mm)		Inst Image Refocus (mm)	Comment
	(0,0)	(0,+2′)	(0,-2′)	(2′,0)	(-2′,0)	dX	dY	dX	dY	dX	dY		Focus only
0	2	13	9	15	13	0	0	0	0	0	0	0	
1	99	99	102	98	100	0.22	-0.20	0.42/0.14%	-0.04/0.01%	2.55	-0.47	0.28	Astig – DM correctable
2	3	16	10	14	11	-0.01	0.02	0	0	0.71	0.06	0.27	
3	7	10	7	20	18	0.02	-0.01	0.02/0.01%	0.01/0.0%	0.31	0.43	0.24	
4	16	25	18	24	16	-0.23	0.42	-0.19/0.06%	0.03/0.01%	-0.64	0.23	-0.41	
5	88	94	90	96	87	1.05	-0.26	-0.15/0.05%	0.02/0.01%	-1.70	0.54	0.03	Astig – DM correctable
6	4	19	13	10	6	-0.05	0.02	-0.01/0.0%	-0.02/0.01%	-0.20	-0.17	-0.33	

2.3 NFIRAOS NRCim – thermally-driven misalignment

In a similar manner to the interface sensitivity analyses, the impact of various system and dome/laboratory temperature combinations were assessed. Specifically, we needed to understand the impact of completing the optical alignment at the I&T facility vs. at the TMT site. Ideally, NFIRAOS could be aligned in the laboratory and then installed at the TMT site without any further alignment required. Table 2 lists the various temperature conditions that were evaluated using NRCim. These thermal disturbances were applied to the FEM to determine the resulting optical perturbations (see Figure 6) which were then piped to ZEMAX via NRCim.

Table 2. Thermal modes evaluated with NRCim

Case	Reference Temp K	Dome Temp K	TABL Temp K
1. At Mauna Kea Alignment, TABL -30	273	273	243
2. At HIA Integration Alignment, TABL -30	293	293	243
3. At MK, HIA Alignment, TABL -30	293	273	243
4. At MK, HIA Alignment, TABL ambient	293	273	273
5. At MK, Operation, Negative Amb. Extreme	273	268	243
6. At MK, Operation, Positive Amb. Extreme	273	282	243

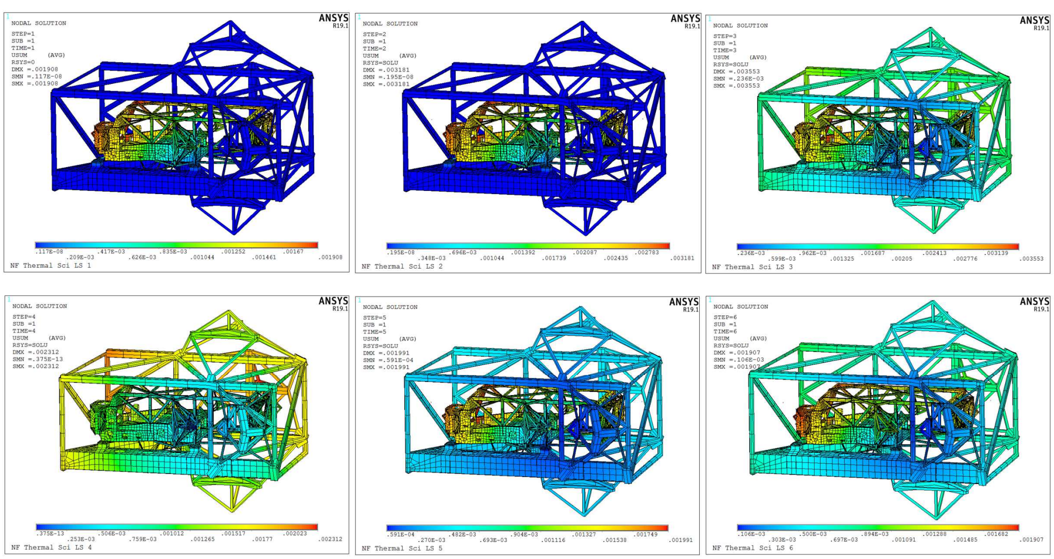

Figure 6. FEA results of thermally-driven structural displacements.

Unlike the alignment sensitivity analyses, these thermal analyses were completed for all three optical prescriptions: the science (SCI) path, the natural guide star (NGS) path and the laser guide star (LGS) path. The thermal perturbations of the FEM were the same in all three sets while the prescriptions used during the NRCim initialization were different. Only the results from the SCI path are presented below (see Table 3) but all three sets were evaluated and the resulting system performance variations were shown to be within acceptable limits.

Table 3. NFIRAOS SCI-path optimized thermal modes

Case #	IQ RMS Wavefront Error for λ=1.65 um After focus compensation (nm) Given at five field points					Focal Plane Mask Motion (mm) / Inst motion (mm) After compensation		Pupil Shift on DM0 after compensation [um] / [% of pupil]		Exit Pupil angle after comp [µrad]	Inst shim (mm)	Comments
	(0,0)	(0,+1')	(0,-1')	(1',0)	(-1',0)	dX	dY	dX	dY	X/Y		
0	2	13	9	15	13	0	0	0	0	-1.3/5.6	0	Nominal case
1 – MK-A	4.6	14	7.4	17	15	-2e-6/0.55	2e-6/0.39	1.7/0%	15/0.005%	2.6/8.8	5.4	Shift NF up / over by ~0.5 mm
2 – NRC INT	5.9	17	12	19	18	-7e-6/0.92	5e-6/0.58	2.8/0%	25/0.008%	5.2/10.9	8.9	Shift NF up / over by ~1 mm
3 – NRC-A	5.9	14	8	17	16	-2e-6/0.55	2e-6/0.36	1.7/0%	26/0.009%	3.1/10.6	10.6	Shift NF up / over by ~0.5 mm
4 – NRC-A TABL Amb.	4.1	14	7.3	16	13	0/0.005	-1.4e-3/0.07	0/0%	11/0.004%	-0.8/7.5	5.3	No realignment
5 – MK-A - Oper. T	4.6	14	6.6	17	15	-2e-6/0.46	1e-6/0.34	1.4/0%	15/0.005%	2.0/8.7	5.8	Shift NF up / over by ~0.5 mm
6 – MK-A + Oper. T	4.6	15	9	18	16	-4e-6/0.72	3e-6/0.49	2.2/0%	15/0.005%	3.5/8.9	4.6	Shift NF up / over by ~0.5 mm

3. ADAPTATION OF NRCIM FOR TRANSIENT ANALYSES

3.1 Dynamic opto-mechanical analysis implementation strategy

Extending the capabilities of the NRCim framework to include the opto-mechanical analysis of structural dynamic and instrument vibrations has long been a high priority and was considered a necessary addition to the functionality of NRCim. The upgrade to the NRCim MATLAB code and associated data structure interactions with the connected analysis tools was completed in 2018 to facilitate the evaluation of optical performance in the presence of dynamic system disturbances both internal and external. The updated NRCim "pipeline" allowed transient disturbances, described in the form of time-series displacements, accelerations or forces, to be applied directly to the existing NRCim framework. The disturbances that were considered most critical included the following:

- TEL.STR-to-NFIRAOS interface vibration inputs (vibrations from TMT),
- Internal LGS mechanism vibrations due to sodium-layer tracking,
- Tip/Tilt Stage (TTS) reaction forces
- Cooling system vibrations from thermal enclosure

While a significant effort was required to adapt and validate the NRCim code for transient disturbances, the core functionality remains the same on a time-step by time-step basis: disturbance applied; FEM response calculated; and optical impact assessed.

3.2 Increased fidelity of the FEM dynamic response

Assessing the dynamic performance of NFIRAOS meant that the FEM needed an improved representation of the dynamic behavior of the various opto-mechanical components. For each subsystem shown in Figure 3, there are three interface nodes (IFx) located at the subsystem's interfaces with the TABL. As illustrated in the schematic view below (Figure 7), the static mass of the subsystem (the mass rigidly attached to the TABL) is defined at the base node ( ) connected to the three interface nodes with rigid link elements. The dynamic ("sprung") mass of the subsystem is defined at the dynamic node ( ). If the nominal orientation of the subsystem natural frequency modes are rotated with respect to the global coordinate system (CS), then the nodal CS of the base and dynamic nodes are rotated accordingly. In this case, a third "follower" node is defined for interfacing with the NRCim. This third node ( ) has a token mass, is constrained to move with the dynamic node and reverses the rotation of the nodal CS to the global CS. Although the three "mass" nodes are shown separated for clarity in the schematic view, each of these nodes are located coincident in the model (appears as one node). The static and dynamic nodes are connected with spring and damper elements in each of the six degrees of freedom. The implementation of the dynamics for each subsystem enables NRCim to automatically evaluate the possible amplification or dynamic coupling effects in the overall WFE analysis. The enlarged view in the right side of Figure 7 shows the connection of the static (or base) mass to the dynamic mass with three orthogonal sets of linear spring/damper elements. Not shown are the three sets of rotational spring/damper elements aligned with each orthogonal axis. In ANSYS, the three linear and the three rotational spring/dampers are defined using the ANSYS element type: COMBIN14 spring/damper element. This element type allow for the definition of both linear and rotary stiffness and damping.

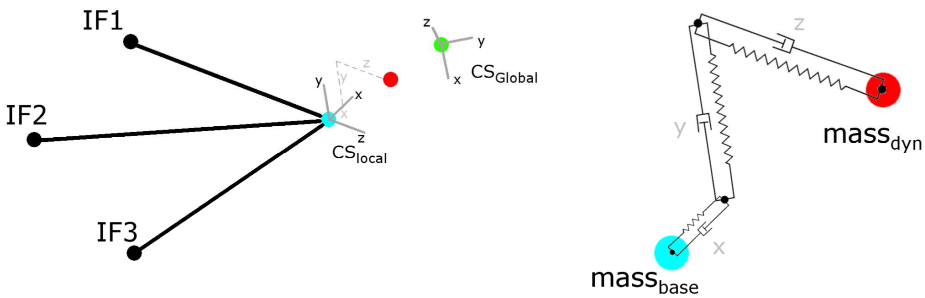

Figure 7. Schematic representation of the subsystem mass decomposition and the addition of spring/damper elements.

The dynamic parameters used to define the subsystem spring/damper elements in the FEM originated from the detailed analyses and final design reports completed for each subsystem in preparation for the NFIRAOS FDR. For each subsystem component within NFIRAOS, the low-frequency modes were included in the NRCim FEM. The modal frequencies and corresponding mode shapes for four of the subsystems are summarized in Table 4.

Table 4. Summary of subsystem modal frequencies and mode shapes used in the transient NRCim analyses.

Subsystem	Modal Freq. (Hz)	Mode Shapes
OAP (1 – 6)	34.5, 48.6	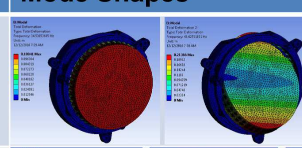
ISM	29.1, 31.8, 45.1	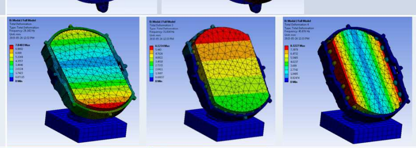
LGS Trombone	54	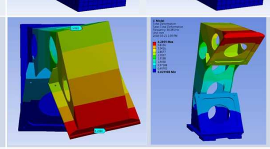
VNW	19, 26	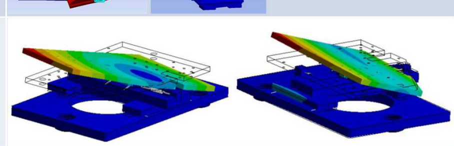

4. TRANSIENT ANALYSES OF NFIRAOS USING NRCIM

4.1 TEL.STR-to-NFIRAOS interface vibration

Three randomly-seeded, orthogonal transient displacement time-series were derived from the TMT-defined interface vibration PSD (see Figure 8) and identically applied to the six NFIRAOS mounting locations (see Figure 4). Note that this effectively dictates that the TEL.STR-NFIRAOS interface moved in translation as a rigid body with zero rotations. The resulting time-series displacement/rotation responses for each optical element were calculated and processed through the transient NRCim pipeline producing a time series of Zernikes describing the time-varying delivered image WFE.

Calculating the open loop RMS WFE variations from the first 12 Zernikes revealed the WFE was almost entirely composed of tip and tilt error (total WFE_{RMS} = 18nm; Tip_{RMS}=8.2nm; $Tilt_{RMS}$=16.1nm). The removal of the tip/tilt error leaves less than 0.07nm RMS of higher order WFE at all field points.

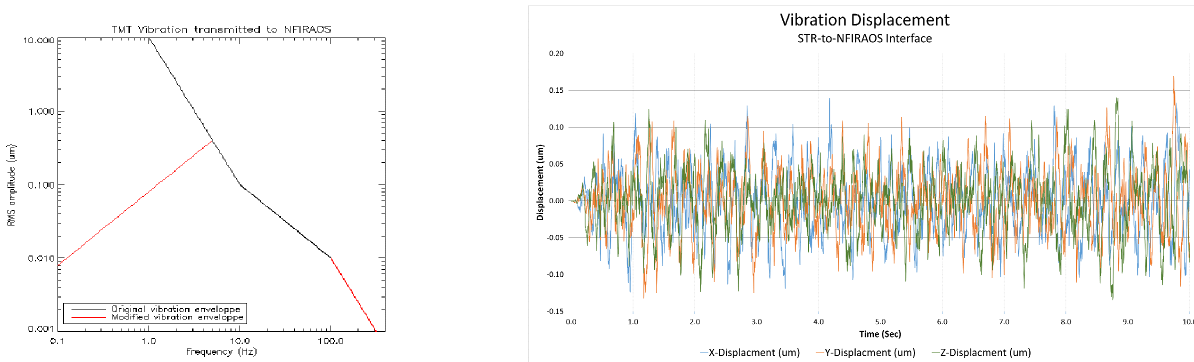

Figure 8. TEL.STR-to-NFIRAOS interface vibration PSD (left) and three displacement time series (right) which were independently derived from the PSD.

The time series of the NFIRAOS delivered image WFE were processed using the NFIRAOS AO rejection transfer function to assess the closed loop AO corrected WFE (see Figure 9). The closed loop WFE is 10nm RMS which is within the allowable WFE budgeted allocated to the TEL.STR Interface vibration: Tip=7.4nm; Tilt=6.7nm;

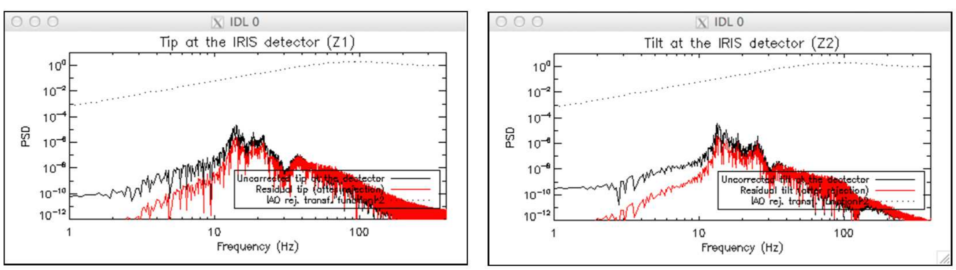

Figure 9. PSD plots for the Tip and Tilt of the delivered image before and after the application of the AO rejection transfer function.

4.2 Dynamic disturbances internal to NFIRAOS

Internal Laser Guide Star mechanism vibrations due to sodium-layer tracking

The NFIRAOS LGS system tracks the variations in the sodium layer. Tracking the various altitude positions requires rapid accelerations and decelerations of the LGS trombone assembly (~230 kg) along a linear stage to maintain the optimal focus. As a results there are inertial reaction forces and moments that are transferred to the TABL. A control algorithm was developed to optimize the tracking performance while limiting the RMS reaction force to less than 0.2 N. The resulting time series of reaction forces (applied to the CG of the trombone assembly) were input into the NRCim to assess the resulting WFE of the delivered Science image which was determined to be 0.03 nm RMS.

Tip/Tilt Stage reaction forces

During normal operation of NFIRAOS, both the tip/tilt stage (TTS) the low-altitude deformable mirror (DM0) assembly operate to correct for tip and tilt errors caused by the following factors:

- atmospheric turbulence,
- telescope windshake,
- telescope vibrations
- WFS noise propagation (estimated to be 1mas RMS of noise propagation)

The two components operate in different frequency ranges and the division between the TTS (low-frequency or “woofer”) and the DM0 surface (higher-frequency or “tweeter”) is implemented using a 20Hz 2nd order high-pass Butterworth filter. Factoring in these operating characteristics, the performance requirements were used to estimate the TTS motions and the resulting time-varying reaction torques applied to the TTS mount. Two randomized versions of these time series were applied to orthogonal axes (X & Y at the face of the DM0 optic)

Using the NRCim Framework as before, the transient perturbations were processed yielding transient changes in WFE. Assessing the WFE for all field positions in the SCI path showed they were all below 0.3nm RMS. Subsequently, the impact to the LGS and NGS IQ was also calculated to be less than 0.3nm RMS

5. FREQUENCY-DOMAIN INTEGRATED MODELING

5.1 Motivation

One deficiency associated with the transient (time-domain) NRCim implementation is the difficulty of incorporating control system characteristics into the dynamic analysis. Using the time-domain NRCim, the estimation of the impact of any control algorithm on the final performance must be done after the transient analyses are completed and cannot fully account for dynamic interactions that may occur as a result of dynamic feedback or similar natural frequencies leading to dynamic coupling. Shifting to a frequency-domain analysis allows for the direct inclusion of control system algorithms and also facilitates conducting integrated modeling across multiple organizations simply by sharing the transfer functions that describe the opto-mechanical performance of each subsystem.

5.2 Frequency-domain integrated modeling (FDim) framework

The strategy developed combines the dynamic structural properties of a system with linear optics models (LOM) to formulate an opto-mechanical transfer function. This is then combined with the input disturbance power spectral density (PSD) to calculate the system performance (illustrated schematically in Figure 10). First, ANSYS harmonic analyses of the FEM are completed to determine the structural response of each optical element to vibration over the desired frequency range (0–400 Hz in the case of NFIRAOS and IRIS → driven by a control system update rate of 800 Hz). This harmonic structural response is a complex matrix characterizing the magnitude and phase of the structural response for the entire frequency range. Next, ZEMAX is utilized to generate a LOM using normalized 6-DOF perturbations of the Zemax prescription describing each part of the system. Finally, as shown in Figure 11, these are combined to give the transfer function for tip/tilt/focus of image at desired location (e.g. WFS, Imager, NGS, or LGS).

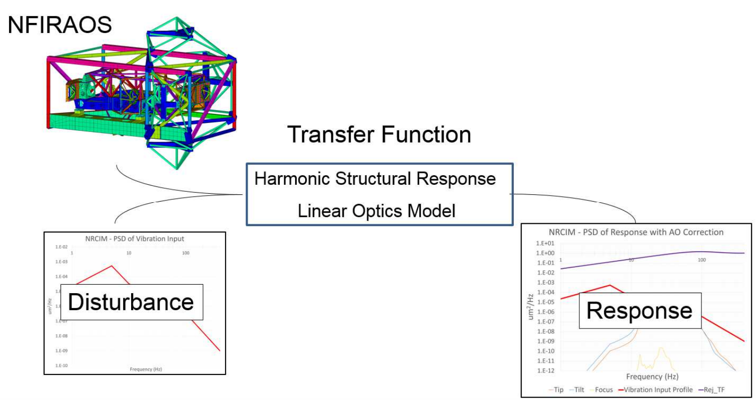

Figure 10. Schematic for frequency-domain analysis procedure.

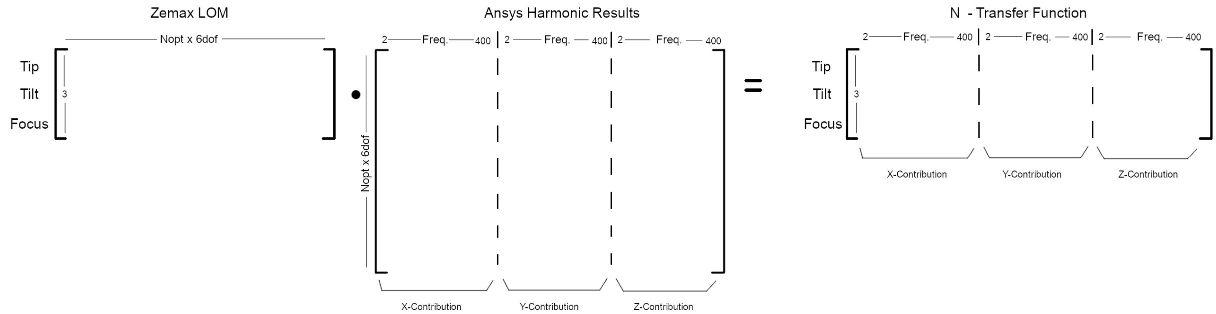

Figure 11. Equation combining the LOM with the harmonic structural response to give the opto-mechanical transfer function.

5.3 FDim Verification

In parallel with the development of the FDim, extensive validation of the code was completed through the use of unit testing and discrete function testing. For one high-level test of the LOM, the transient perturbation data generated by the ANSYS transient analysis was multiplied, for each time-step, by the LOM and compared to the NRCim (transient) results showing that they were numerically identical and confirming that the LOM is returning exactly the same WFE prediction as the ZEMAX prescription.

The final verification step was to convolve the full transfer function with the PSD of the input vibration to calculate the RMS tip, tilt and focus. As shown in Figure 12, the PSD input disturbance is repeated for all three orthogonal directions and multiplied, element-wise, by each row of the modulus of the transfer function [N] resulting in the Response PSD (Figure 13). The RMS tip, tilt and focus can then be calculated using the formula given below:

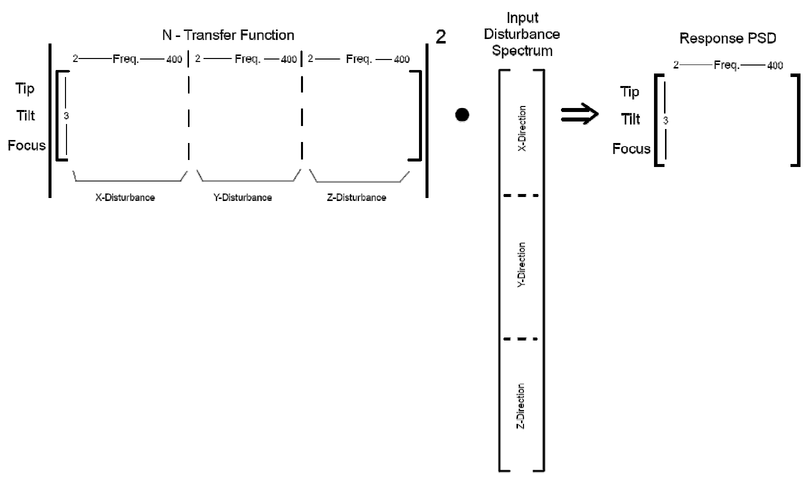

$$RMS_{TTF} = \sqrt{\sum_{0}^{400}[Resp_{PSD} \cdot \Delta f]}$$

Figure 12. Equation used to calculate the PSD response (and subsequent RMS) given an input disturbance PSD

A comparison of the RMS results shows very good agreement between the time-domain and frequency-domain methods:

- NRCim: Tip=8.2nm; Tilt=16.1nm; Focus=0.05nm
- FDim: Tip=8.3nm; Tilt=15.7nm; Focus=0.05nm

Similarly, the results following the application of the AO Rejection transfer function were the same as those predicted using the time-domain method: Total RMS_{WFE}=10nm with RMS_{Tip}=7.4nm and RMS_{Tilt} =6.7nm.

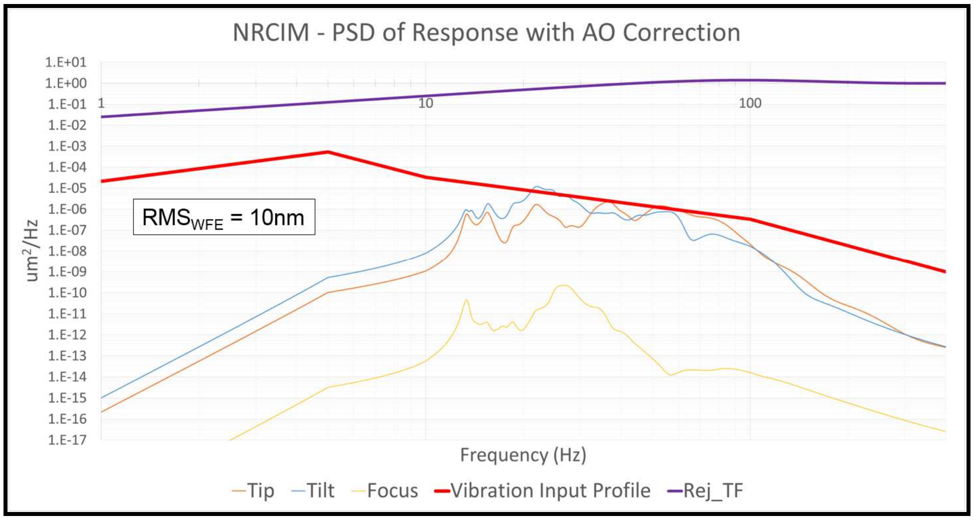

Figure 13. **Dynamic optical performance in the presence of telescope vibration after convolution with the AO rejection transfer function.**

6. NFIRAOS/IRIS FREQUENCY DOMAIN INTEGRATED MODELING (NIFDIM)

6.1 Application to NFIRAOS and IRIS

Upon completion of the FDim framework development and testing, this technique was used to predict the performance of NFIRAOS with IRIS mounted on the NFIRAOS bottom instrument port. The measurements from the IRIS on-instrument wave front sensors (OIWFS) are used by the NFIRAOS RTC to control the TTS and DM0 inside NFIRAOS. The transfer functions required to complete this analysis are shown schematically in Figure 14 and listed below:

- [N] is the opto-mechanical transfer function from the TEL.STR interface to the NFIRAOS delivered image focal plane.
- [A] is the structural transfer function from TEL.STR interface to the NFIRAOS/IRIS interface (assumed to be unity since the IST is very stiff in this region).
- [B] is the opto-mechanical transfer function from the NFIRAOS /IRIS interface to the IRIS science imager
- [C] is the opto-mechanical transfer function from the N NFIRAOS F/IRIS interface to the IRIS OIWFS imager

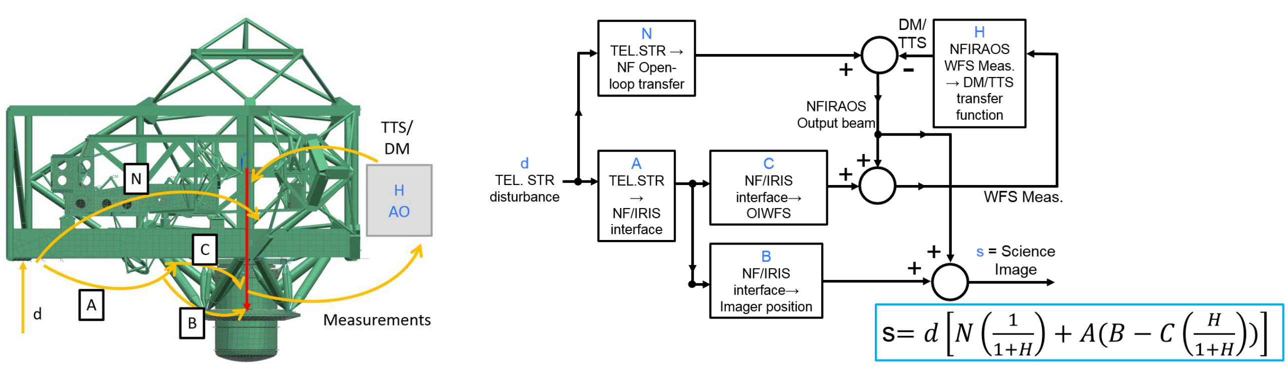

Figure 14. **Graphical representation of the transfer functions required to combine NFIRAOS and IRIS (left) and the control flow chart for NFIROS and IRIS (right).**

A simplified IRIS FEM was distilled from a highly-detailed FEM while maintaining all of the fundamental vibration modes except for those associated with the science cryostat vibration modes. The full [B] transfer function was provided separately. While the full cryostat is not represented in this FEM, the mass and moment of inertia properties are included in a lumped mass node (identified as the target of transfer function [B] in Figure 15). The transfer function [C] was computed and used in the NIFDim analysis to calculate the OIWFS portion of the system performance. The total WFE at the OIWFS imager was 0.4nm RMS (Tip=0.2nm; Tilt=0.4nm; Focus=0.1nm). The full transient (NRCim) analysis was also completed for the IRIS FEM yielding identical results further validating the NIFDim framework.

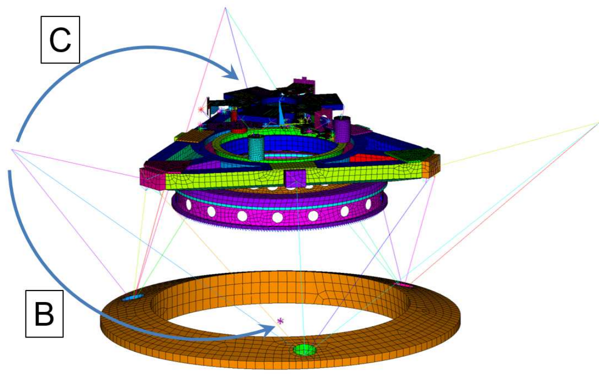

Figure 15. FEM used to calculate the IRIS OIWFS imager transfer function.

7. CONCLUSION

The NRCim framework, used in the design of several previous projects, was implemented in the design of NFIRAOS to evaluate the optical impact of several static perturbation. The NRCim framework was then expanded and enhanced to facilitate the evaluation of system performance metrics in the presence of complex dynamic disturbances. This technique was used to evaluate the NFIRAOS performance while exposed to real-world telescope vibration and showed that the WFE of the delivered image will be limited to 10nm RMS. Several other internal vibration sources were also evaluated and shown to have even less impact on the final delivered image quality.

Since NFIRAOS must meet specific performance targets with client instruments attached and there was a need to incorporate control system effects in the overall system performance, NRCim was modified to operate in the frequency-domain. The NFIRAOS/IRIS Frequency-Domain integrated model (NIFDim) framework was developed and validated through comparisons with NRCim results. NIFDim was used to evaluate various aspects of the NFIRAOS/IRIS combined system and will be used to further assess the nature of their dynamic interaction and combined performance.

REFERENCES

[1] Pazder, J., Roberts, S., Smith, M., Lavigne, J.-F., McKenzie, H. “The optical modeling tools for the Canadian Very Large Optical Telescope Integrated Model”, Proc. SPIE Vol. 5382, p. 404-412, Second Backaskog Workshop on Extremely Large Telescopes, (2003); https://doi.org/10.1117/12.566266

[2] Roberts, S., Pazder, J., Fitzsimmons, J., Herriot, G., Loewen, N., Smith, M., Dunn, J., Saddlemyer, L. “Integrated Modeling of the Canadian Very Large Optical Telescope”, Proc. SPIE Vol. 5382, p. 346-355, Second Backaskog Workshop on Extremely Large Telescopes, (2004); https://doi.org/10.1117/12.566206

[3] Roberts, S., Sun, S., Kerley, D. “Optical performance analysis and optimization of large telescope structural designs”, Proc. SPIE Vol. 5867, p. 200-211, (2005); https://doi.org/10.1117/12.618568

[4] Roberts, S., "NRCIM integrated opto-mechanical analysis toolset for the Thirty Meter Telescope", Proc. SPIE 8336, Integrated Modeling of Complex Optomechanical Systems, 83360A (2011); https://doi.org/10.1117/12.914555

[5] Erickson, D., Roberts, S., Pazder, J., Fletcher, J. M. "Integrated modeling for the GPi flexure sensitive structure", Proc. SPIE 7017, Modeling, Systems Engineering, and Project Management for Astronomy III, 701711 (9 July 2008); https://doi.org/10.1117/12.788449